Design, development, and performance evaluation of a drum-type electrical powered cassava peeler

Amana Wako[1*], Bisrat Mekonnen[1], Mustefa Jarso[2]

(1. Department of Mechanical Engineering, Adama Science and Technology University, Adama, 1888, Ethiopia;
2. Department of Agricultural Engineering, Haramaya Institute of Technology, Haramaya University, Dire Dawa, 138, Ethiopia)

Abstract: Cassava (Manihot esculenta) is one of the most important tuber crops, constituting a considerable portion of the daily diet of people in southern Ethiopia. Currently, the production of plants is being increased to alleviate food insecurity. However, the manual operation of cassava tuber peeling is so arduous to change for food staff. The main objective of this study was therefore to design, develop, and evaluate the performance of an electrically powered cassava peeler machine. Physical properties of the cassava crop were determined as input for machine design. During the designing and development of the peeler machine, material selection, the strength of materials, engineering properties, and the theory of machines and mechanisms were considered. Based on the engineering properties of the cassava crop, machine components were designed, including a cylindrical peeling drum, drum cover, plate, shaft, pulley, peeling machine supporting frame, and belt. Split-plot experimental design at two levels of drum speed, which require low and high-speed levels for different sizes and maturity of cassava crop, and three levels (low, medium, and high capacity) of percentage drum fill were used to test the machine; and collected data were analyzed using SPSS statistical software. The result shows that peeling efficiency machine is 94.8667% at a drum speed of 60 rpm and 10% fill, flesh loss is 7.8% at 60 rpm drum speed and 10% drum fill, and 120 kg h^{-1} throughput capacity at 60 rpm drum speed and 20% drum fill. The developed machine needed to be evaluated at a higher percentage drum fill, peeling drum speed, and retention time. The future studies should evaluate other factors such as tuber size, peeling duration, and blade type to enhance the overall performance, and the cost-benefit analysis should be conducted to determine the economic feasibility of different operational settings.

Keyword: cassava peeling machine, mechanical design, performance evaluation, small-scale processing, Ethiopia

Citation: Wako, A., B. Mekonnen, and M. Jarso. 2026. Design, development, and performance evaluation of a drum-type electrical powered cassava peeler. Agricultural Engineering International: CIGR Journal, 28(1):202-220.

1 Introduction

Cassava is a prominent food in tropical regions, including Asia, Africa, and Latin America. It is an important diet for about 500 million people across the globe. Among tropical food crops, Cassava is the fourth most important crop for farmers in the tropics after rice, wheat, and sugarcane, and produces more than 250 million tonnes of fresh roots each year (Scaria et al., 2023). In sub-Saharan Africa (SSA), cassava is mainly a subsistence crop grown for food by small-scale farmers who sell the surplus. It grows well in poor soils with limited labor requirements. In Ethiopia, cassava is one of the important root and tuber crops supporting a considerable portion of the Ethiopian population. It is grown by small-scale subsistence farmers under resource-poor conditions and used as a major staple diet in the south, southwest,

Received date: 2025-04-14 **Accepted date:** 2025-11-18

***Corresponding author, Amana Wako.** Department of Mechanical Engineering, Adama Science and Technology University, Adama, Ethiopia. Email: amalowak2014@gmail.com.

eastern, and northwest parts of the country (Sarka et al., 2017).

It was believed that cassava was introduced by some NGOs to drought-prone areas of the southern part of the country, such as Amaro, Gamogoffa, Sidama, Wolayta, and Gedeo, primarily to fill the gap for subsistence farmers due to failure of other crops as a result of drought. In these areas, farmers usually grow cassava in small, irregular, scattered plots either sole or intercropped mainly with enset, maize, and sweet potato.

The average total coverage and production of cassava per annum in the southern region of Ethiopia is 4,942 hectares with a yield of 53,036.2 tons (Markos et al., 2016). Its use as a potential food crop in Ethiopia has been appreciated since the 1984 famine (Amsalu, 2006). Compared to cereal crops, cassavas are high-yielding yielders, environmentally friendly and are staples that provide low-cost energy to the human diet. Therefore, cassavas have significant contributions towards food security, income generation, resource base conservation, and ensuring sustainable food availability throughout the year (Immanuel et al., 2024).

According to Sakadzo et al. (2025), Cassava is referred to as a food security crop, which can be left in the ground for extended periods of up to two years, until required. It is also one of the most important starchy foods, and its tuberous roots are a valuable source of cheap calories, especially in developing countries like Ethiopia, where calorie deficiency and malnutrition are widespread. One essential quality of cassava's root that has made it an important food security crop, mostly among low-income countries, is its ability to grow well in poor soil. Another important quality is its inherent ability to remain in the soil for a long period after maturity without undergoing any degradation (Tobiloba et al., 2019).

According to Sarka et al. (2017), four types of Ethiopian traditional recipes with two levels of cassava blended with cereals at a proportion of 50% and 70% are injera, dabo (bread), anebabero, and porridge. Cassava requires considerable post-harvest labor because the roots are highly perishable and must be processed into a storable form soon after harvest. The cassava plants are generally categorized as bitter and sweet, depending on their cyanide content. The low-HCN, or sweet cassava, has less than 50 ppm of cyanogen equivalents, while the high-HCN, or bitter cassava, has more than 100 ppm (Wilson and Dufour, 2002).

Chemically, cassava is composed of water (60%-70%) and starch with minor amounts of protein, fiber, minerals, vitamins, and toxic components of cyanogenic glucosides. The presence of this toxic component requires a special processing procedure to make the product safe for human consumption. Initially, harvested cassava tubers must be peeled to remove the inedible outer parts of the root, consisting of the corky periderm and the cortex, which are known to contain most of the toxic components. Then, hydrogen cyanide is considerably reduced and drives off during slicing, grating, and subsequent processing stages. Thus, proper processing is indispensable to use cassava safely as a healthy diet for the majority of the population (Ukonu et al., 2022; Kanaabi et al., 2024).

Cassava peeling is the first and most important activity in the overall cassava processing line, and failure of adequate peeling will result in health problems in human beings as the major percentages of hydrogen cyanide, which is responsible for the toxicity of cassava, are found in corky periderm and cortex (Ertebo and Koroso, 2024). Most of these operations are still being done manually, especially peeling, and they are generally labor-intensive, arduous in nature, time-consuming and unsuitable for large scale productions because of its low output (Gezahegn and Bazie, 2021; Davies et al., 2008).

Mechanization of the cassava peeling process will significantly increase the rate of production, quality of products, and their availability (Aniedi et al., 2012). Peeling involves the removal of a thin layer from a stock. Removing peels of cassava tubers is imperative, to avoid the concentration of cyanogenic glucosides responsible for cassava toxicity is highest in cassava

peels (Ertebo and Koroso, 2024). Cassava peeling is an irreplaceable unit operation in the processing cycles of cassava tubers to obtain their various desired products. Among other processes, peeling is the most difficult of all unit operations because, by nature, harvested tubers have variations in sizes and shapes.

In the Ethiopian context, cassava peeling is done using a knife, usually by women and children, because of the absence of cassava peeling machines. The equipment used for the traditional peeling is cheaper compared to modern high technology; however, there is a high risk of injury or low output. This traditional peeling results in low yield, is time-consuming, and is labor-intensive. Thus, developing a cassava peeling machine that will satisfactorily peel the tubers with reduced tuber loss is highly important. Therefore, the main objective of this study was to design, develop, and evaluate the performance of an electric-powered cassava peeler machine.

2 Materials and methods

2.1 Study site description

The study site where the design, development, and performance evaluation of the cassava peeling machine was conducted is located, as indicated in Figure 1, in Oromia Regional State, Adama Woreda, in East Sha Zone, near the town of Awash-Melkassa, 117 km East of Addis Ababa and 17 km southeast of Adama city at Melkassa Agricultural Research Center (MARC). It is found at an altitude of 1466 m above sea level and lies on the geographical coordinates of 8°24'0" N, 39°20'0" E Latitude and Longitude respectively.

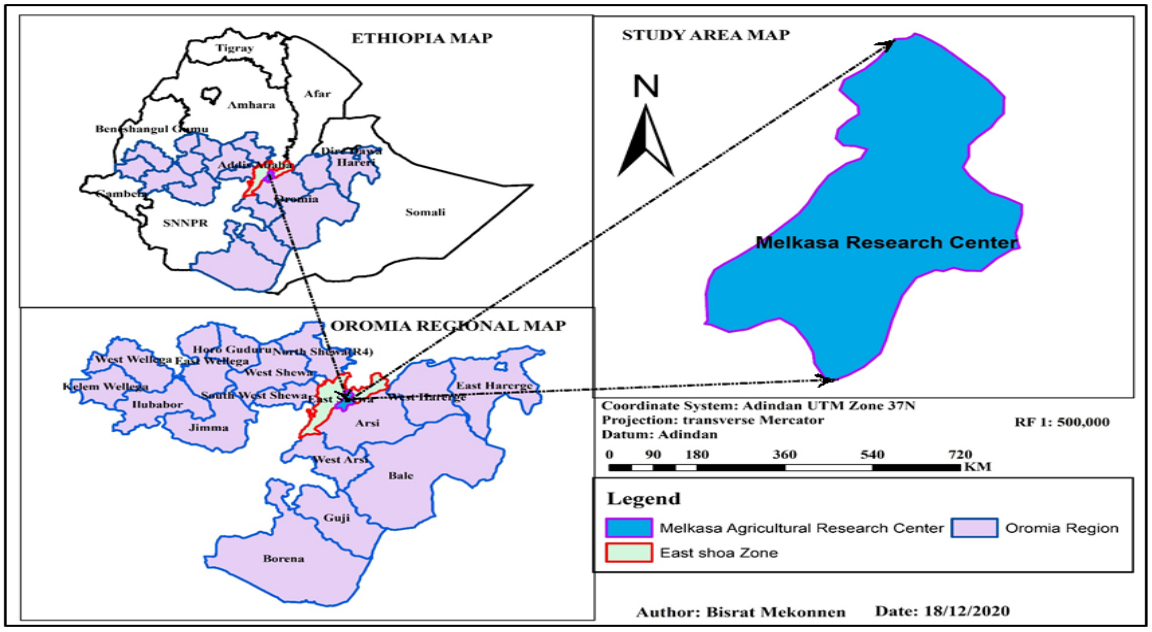

Figure 1 Study site map

Fabrication of the prototype and any adjustment or maintenance was also conducted in the Agricultural Engineering Research workshop, which was found in MARC.

2.2 Materials

During the design and development of the machine, the strength of materials, engineering material science, and the theory of machines and mechanisms were considered. Since cassava is a food for human beings, the quality of the food as well as the durability of the material for the construction of the peeling machine was put into consideration (Alhassan et al., 2018). To preserve the quality of food, fabrication materials should possess the ability to withstand corrosion, wear and tear. In addition to the aforementioned issues, affordability, availability, and strength of the materials for construction, as well as physical properties of the materials to be peeled, were given due consideration (Alhassan et al., 2018). The materials selected for the constructions were based on ease of fabrication, toughness, machinability,

availability, and cost. During the construction of parts of the machine that have direct contact with the cassava tubers, like the drum, a great concern was given to food contamination. Accordingly, the drum was constructed of stainless steel. Whereas other parts like frame, drum cover, and protective hood were constructed from high-thickness and strength materials by considering the durability of the developed machine. The sample of cassava tuber was collected from MARC and farmers of Wolayta zuria woreda.

Different tools and instruments indicated in Figure 2 were used to carry out different measurements on the cassava root tubers. A tape rule was used to measure the length of cassava tubers while the diameter of the cassava tubers was measured by using a digital caliper. The weight of cassava tubers, cassava peeler and flesh loss were measured with an electronic weighing balance with accuracy of 0.10g. The time of operation was recorded using a mobile stopwatch application while partially peeled cassava peels were removed by a knife manually.

Figure 2 Measuring instruments for cassava tuber

The three principal dimensions, namely major, minor and intermediate diameters of sampled tubers were measured using digital caliper with an accuracy of 0.01 mm and measuring range of 0.00-150.00 mm. Some of physical properties needed for design of cassava peeler are discussed below.

2.3 Determination of physical properties

2.3.1 Moisture content

The moisture content of sliced cassava tubers was determined using the oven dry method. The weight of the cassava tuber was measured using a digital balance with a capacity of 15.00 kg and an accuracy of 0.01 g. The sliced sample weight was recorded before and after oven-drying at 105°C until a constant weight was obtained. The mean values of moisture content were calculated to be 55.3% using Equation (1) (Ndirika and Oyeleke, 2006).

$$\mathrm{Mc} = \frac{\mathrm{Ww\text{-}Wd}}{\mathrm{Ww}} \times 100 \qquad (1)$$

Where,

W_w is the weight of the wet sample (g);

W_d is the weight of the dried sample (g);

M_c is the moisture content on a wet basis.

2.3.2 Thickness

The thickness of peeled and unpeeled cassava tubers was determined using a digital vernier caliper. These were done at the major diameter (head) taken as “a,” intermediate diameter (middle) as “b,” and minor diameter (tail) as “c.”. The main concern in determining the thickness of the cassava tuber was all about specifying the clearance between the plates made the drum. The mean values of GMD for unpeeled cassava tubers were calculated to be 19 mm using Equation (2) (Ehiem and Simonyan, 2012).

$$\mathrm{GMD} = \sqrt[3]{\mathrm{a\ b\ c}} \qquad (2)$$

Where,

GMD is Geometric mean diameter (mm);

a is Major diameter (mm);

b is Intermediate diameter (mm);

c is Minor diameter (mm).

2.3.3 Sphericity

The shape of agricultural material is usually expressed in terms of its sphericity. Sphericity, or shape factor, is the degree to which an object looks a lot like a sphere. The sphericity of cassava tuber was

determined by the result obtained from GMD and the major diameter "a" using Equation (3) (Koocheki et al., 2007). The mean value of sphericity was therefore; calculated to be 1.3.

$$\text{sphericity}=\frac{\text{GMD}}{\text{a}} \quad (3)$$

2.3.4 Mass and volume

The mass of cassava tubers was weighed by a digital weighing balance with an accuracy of 0.1 g and a capacity of 15 kg. The volume of cassava tubers was determined by water displacement methods in such a way that the container was filled with water up to the top and then placed in another container. The cassava tuber was then totally immersed in the container, and the amount of water displaced was used to determine the volume of cassava tubers (Hughes, 2005).

2.3.5 Bulk Density

The bulk density of tubers was determined by weighing the tubers packed in a container of known weight and volume; the container, having a volume of 18 liters and a mass of 0.5 kg was totally filled by cassava tubers in a way that it was at the top level of the container. Then the container, together with samples of cassava tuber, was weighed by a weighing balance with an accuracy of 0.01 g and a capacity of 15 kg to be 12.5 kg. The bulk density of cassava tubers was calculated to be 666.67 kg m^{-3} using Equation (4) (Rao et al., 2014).

$$\rho b = \frac{\text{Mbl}}{\text{Vc}} \quad (4)$$

Where,

ρ_b is the Bulk density of the tubers (g cm^{-3});

M_{bl} is the Bulk mass of the tubers (g);

V_c is the Volume of the container (cm^3).

2.4 Description and design of cassava peeler machine

2.4.1 Parts and description of cassava peeling machine

The parts of the developed cassava tuber peeler include a peeling drum, a drum cover, a protective hood, bearings, a belt and pulleys, a motor setup for a power source, and a mounting frame. The peeling unit is a cylindrical drum having a diameter of 506 mm and a length of 600 mm. It was constructed from 20 pieces of perforated stainless-steel plates that are equally spaced. The space between each plate made the drum wide enough to let out the cassava peels while narrow enough to retain the smallest peeled cassava tuber in terms of thickness or diameter.

The peeler has a prime mover 1 hp electric motor rotating at a speed of 1450 rpm, and a speed reducer having the capacity of a 50 to 1 rpm assembly that is aligned with the shaft of the peeling drums and mounted on the frame and motor setup. The developed machine was constructed in such a way that the frame and motor setup were easily connected by a bolt and nut, which made it easy for transportation and moving from place to place. The protective hood was used to guide the peels to the delivery opening and also to prevent the splash of dust and peels to the operator and motor. The materials that were used to develop the cassava peeling machine were square hollow section, round bar, angle iron, flat iron, cylindrical hinges, iron pipe, mild steel sheet metal, stainless steel sheet metal, bolts and nuts, pulleys and belts, and bearings, as shown in Figure 3 below. Every component of the cassava peeler machine would be fabricated in such a way as to give strength and stability to the system during operation for efficient output.

2.4.2 Operational description of cassava peeler machine

The conceptual view of a machine shows how the corky periderm and cortex would be removed without significant loss of the starchy flesh of the cassava tuber. The machine consists of a cylindrical drum that was made of perforated stainless steel. The drum was supported by a pillow bearing bolted with a hollow square section frame, which permits the set of perforated stainless-steel plates to rub against the cassava tubers, and meanwhile, the cassava also rubs against each other.

The peeling operation began with the rotating motion of the peeling unit through the belts and pulleys that obtained power from the prime mover. The speed reducer (50:1) was used to reduce the

speed of the prime mover through belts and pulleys to bring about a convenient speed of the peeling drum. Cassava tubers were batch-fed into a cylindrical drum, and the rotation was started by a motor. The peels of cassava left the drum through the clearance left between each plate and made the drum drop collectively through the outlet opening.

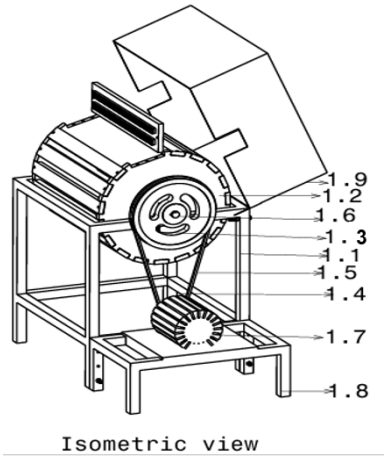

1.1. Frame
1.2. Drum
1.3. Shaft pulley
1.4.Motor ulley
1.5. Belt
1.6. Shaft
1.7. Motor
1.8.Motor frame
1.9. Cover

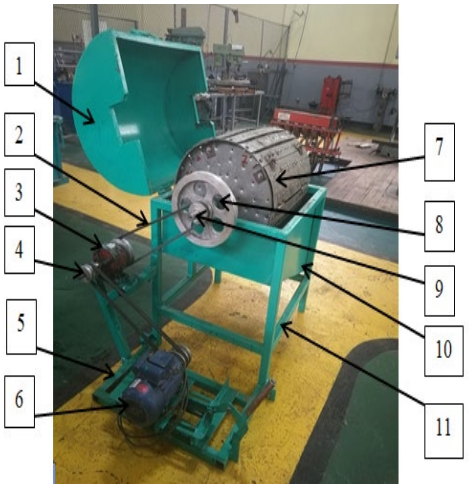

1. Drum cover, 2. Belt, 3. Speed reducer gear, 4. Pulley, 6. Prime mover (1hp electric motor), 7. Drum, 8. Bearing, 9. Shaft, 10. Peels protective hood and 11. Frame.

Figure 3 Developed cassava peeling machine

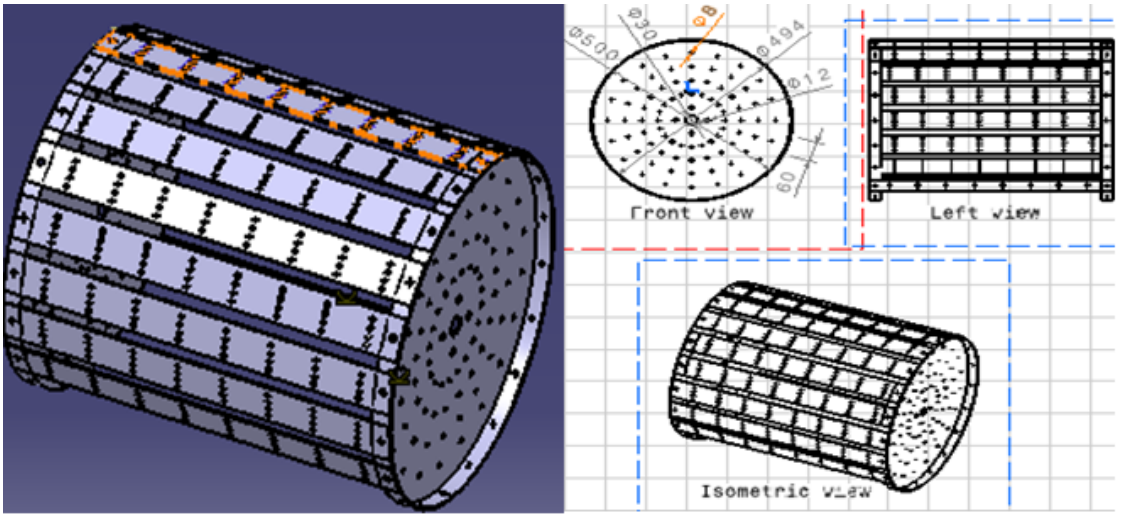

Figure 4 Cylindrical peeling drum

2.5 Design of cassava peeling machine component

The major design analysis was done on the drum, shaft, and pulley. Other parts of the machine that were included in the design were the frame, motor setup, drum cover, and protective hood that guides peels to the outlet. The remaining parts of the machine that were not designed like a belt, bearing, and speed reducer were selected based on the standard.

2.5.1 Drum design

The peeling unit, as shown in Figure 4, is a cylindrical drum; diameter and length are determined based on the prime mover, the desired capacity of the peeling unit, and the compactness of the machine. The drum was made of a set of perforated stainless-steel plates of 3 mm thickness arranged in a cylindrical manner. According to Khurmi and Gupta (2005), the volume of the hollow cylinder was determined using Equation (5). The volume of the peeling drum was determined based on the capacity of 120 kg hr^{-1} of the cassava peeling machine. The volume peeling drum of 0.011 m^3, 0.0167 m^3, and 0.022 m^3 corresponding to the machine capacity 60 kg hr^{-1}, 80 kg hr^{-1}, and 120 kg hr^{-1} respectively, were determined. For the drum having an outer diameter of 0.506 m, an inside diameter of 0.007 m, and a height

of 0.55 m, the volume was calculated to be 0.111 m³.

The volume of the peeling drum was designed for a maximum capacity of 600 kg hr^{-1}, which was equivalent to 100% of the peeling drum filled by the cassava tuber by volume. But for properly peeling the tubers and to avoid clogging, the volume of unpeeled cassava tubers within the peeling drum needed to be about 20% of the total volume of the drum, which is equivalent to 0.022 m³. To know the number of stainless-steel sheet metal plates that made the drum, use the circumference of the circle and divide by the width of the plate by considering the clearance between the plates made by the drum as Equations (6) and (7), respectively. Accordingly, the circumference of the drum and the number of plates used to make the drum were calculated as 1.571 m and 20 pcs, respectively.

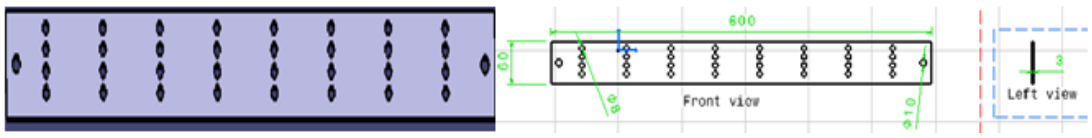

Figure 5 Design of plate

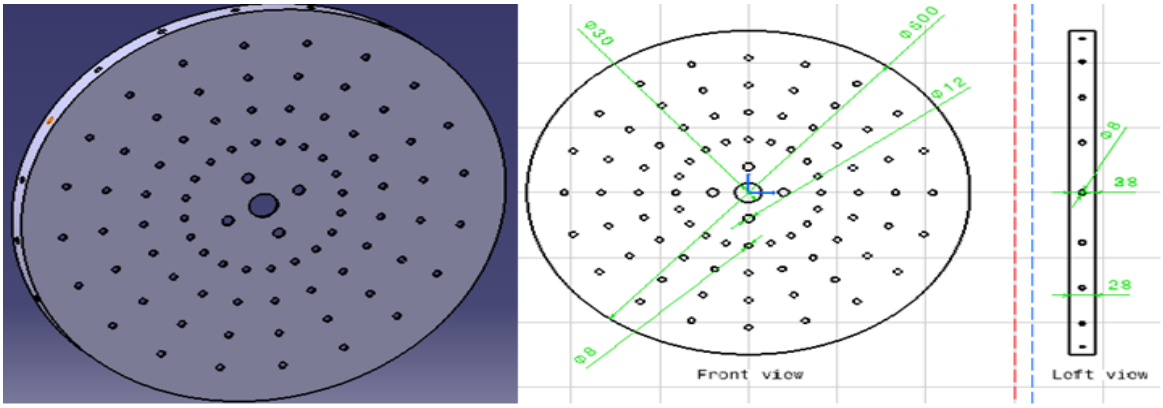

Figure 6 Design of circular plate

$$V = \frac{\pi}{4}(d_o^2 - d_i^2) \times L \quad (5)$$

Where,

V is Volume of the peeling cylinder (m³);

d_i is Inside diameter of the peeling cylinder (m);

d_o is Outside diameter of the peeling cylinder (m);

L is Length of the cylinder (m).

$$C = 2\pi r \quad (6)$$

$$No = \frac{C}{W} \quad (7)$$

Where,

C is the circumference of the peeling drum (m);

r is the radius of the drum (m);

w is the width of the plates made of the drum (m);

No is the number of plates.

2.5.1.1 Design of plates

The plate was rectangular in shape (see Figure 5); therefore, the rectangular structural formula using Equation (8) was used to calculate the volume of a single plate, which was 10.8×10^{-5} m³.

$$Vp = L \times w \times t \quad (8)$$

Where,

L is the length of the plate (m);

w is the width of the plate (m);

t is the thickness of the plate (m);

Vp is the volume of the plate (m³).

2.5.1.2 Design of circular plates

For the two ends closing the drum, circular stainless sheet metal was used, and its volume was determined as 5.89×10^{-4} m³ for a single plate using Equation (9) as shown in Figure 6.

$$Vcp = \pi r^2 t \quad (9)$$

Where,

r is the radius of circle (m);

t is the thickness of the plate (m);

Vcp is the volume of the circular plate (m³).

From Equations (10) and (11), the mass of the plate made of the drum can be calculated by using the

volume and density; for stainless steel, the density was 7,700 kg m^{-3}. Therefore, for 20 rectangular plates and 2 circular plates, the mass was calculated as 15.24 kg and 9.06 kg, respectively.

$$M_p = \rho \times V_p \quad (10)$$

$$M_{cp} = \rho \times V_{cp} \quad (11)$$

Where,

Mp is the mass of the plate (kg);

Mcp is the mass of the circular plate (kg);

ρ is the density of stainless steel (7,700 kg m^{-3});

Vp is the volume of the plate (m^3);

Vcp is the volume of the circular plate.

The total mass was therefore the sum of the mass of the stainless-steel plate (15.24 +9.06) kg, the mass of the cassava tuber (15 kg), and the mass of bolt and nuts (2.5 kg), which was equal to 41.8 kg.

The force "F" required to peel cassava by the drum of mass "m" having a tangential acceleration "a" is given by Newton's second law as Equation (12).

$$F = ma \quad (12)$$

Where,

F is the force required to peel cassava tubers (N);

m is the mass of the drum together with cassava tubers (kg);

a is the tangential acceleration of the drum (m sec^{-1}).

From the equation of motion, it's known that $v = u + at$; since the drum is turning at an average constant speed by the time the peeling begins, the initial speed "u" is zero. Then Equation 12 is rewritten as Equation (13).

$$F = m\frac{v}{t} \quad (13)$$

The angular speed "v" was given by the Equation (14).

$$v = \frac{2\pi rN}{60} \quad (14)$$

Substituting Equation (14) into Equation (13), the force required to peel cassava tubers was given by Equation (15).

$$F = m\frac{2\pi rN}{t} \quad (15)$$

Using Equation (15), the force required to peel cassava tubers was calculated as 3.824 N.

Where,

F is the force required to peel cassava tubers (N);

m is Mass of drum (kg), *t* is time (sec);

N is speed of drum (rpm) and *r* is the radius of the peeling drum (m).

The normal force, the torque, angular velocity, and power required to peel cassava tubers were determined as 3.824 N, 0.967 Nm, 6.284 rad s^{-1}, and 6.007 W using Equations (15)-(18) (Khurmi and Gupta, 2005), respectively.

$$T = Fr \quad (16)$$

$$\omega = \frac{2\pi n}{60} \quad (17)$$

$$P = T\omega \quad (18)$$

Where,

P is power required (watts);

T is torque required to drive peeling drum (N-m);

w is angular velocity (rad s^{-1});

n is speed of peeling drum (rpm);

r is radius of peeling drum (m).

2.5.2 Shaft design

The design of shafts (Figure 5) was based on strength and makes use of the maximum shear stress theory, or Guest's theory. Shafts must be designed so that deflections are within acceptable levels. The diameter of the shaft subjected to a fluctuating load (load due to rotational speed variation) was estimated using Equation (19) (Khurmi and Gupta, 2005). According to ASME code for rotating shafts, when the load was applied with minor shock, the value of Kb is 1.2 to 2.0, and Kt is 1.0 to 1.50. Furthermore, it was noted that for a shaft without a keyway, the allowable stress τ must be 55 MN m^{-2}, and for the shaft with the keyway, the allowable stress τ should not exceed 40 MN m^{-2} (Khurmi and Gupta, 2005).

$$d^3 = \frac{16}{\pi\tau all}\sqrt{(KbMb)^2 + (KtT)^2} \quad (19)$$

Where,

d is the diameter of the shaft (mm);

τall is the allowable stress (N m^{-2});

kb is the combined shock and fatigue factor applied to the bending moment;

Mb is the bending moment (N-m);

kt is the combined shock and fatigue factor applied to the torsional moment;

T is the torsional moment (N-m).

The amount of torque exerted on the shaft by the electrical motor of 1 hp (horsepower) and a speed of 1450 rpm was determined as 4.912 Nm by using Equation (20) (Khurmi and Gupta, 2005). But the maximum torque was 25% greater than the calculated torque and can be equal to 6.14 Nm.

$$T = \frac{60\ P}{2\Pi N} \quad (20)$$

Where,

P is Power (kW);

N is Speed (rpm);

T is Torque (Nm).

The torque and tension, both on the motor side and the drum side, were calculated because of the presence of a speed reducer between the motor and the drum. So that the drum side torque and tension were used in the determination of the shaft diameter.

The torque exerted on the driven pulley was given by Equation (21) (Khurmi and Gupta, 2005).

$$T = (T_1 - T_2)\ r_2 \quad (21)$$

Where,

T_1 is Tension in the tight side of the belt in motor side (N);

T_2 is Tension in the slack side of the belt in motor side (N);

r_2 is Radius of driven pulley (m).

Wrap angle and angle of lap for an open belt are calculated using Equations (22) and (23), respectively.

$$\sin\alpha = \frac{r1\text{-}r2}{x} \quad (22)$$

$$\theta = (180\text{-}2\alpha)\frac{\pi}{180}\text{rad} \quad (23)$$

Where,

r1 is the radius of the drive pulley (mm);

r2 is the radius of the driven pulley (mm);

x is the center distance between the two pulleys (mm);

α is the warp angle (°) and is the angle of lap.

By taking the center of distance between the pulley and speed reducer 0.5 m from both the motor and drum side due to the suitability of construction, the wrap angle (and angle of lap) is obtained as 2.0630 and 3.07 rad, respectively.

The belt tension equation can be determined using Equation (24).

$$2.3\log\left(\frac{Tt}{Ts}\right) = \mu\ \theta \quad (24)$$

Where,

Tt is the tension in the tight side of the belt (N);

Ts is the tension in the slack side of the belt (N);

μ is the coefficient of static friction between the belt and pulley;

θ is the lap angle (°).

From the belt tension Equation (24), $2.3\log\left(\frac{T1}{T2}\right) = \mu\ \theta$.

Taking the coefficient of static friction between the aluminum pulley and rubber belt as 0.3, *T1* and *T2* are calculated as 317.36 N and *T2* = 126.24 N, respectively.

The power required to rotate the shaft was determined to be 5.53 watts according to Equation (25).

$$P = m_{sh} g r_{sh} \omega \quad (25)$$

Where,

P is power required to rotate peeling drum and shaft (watts);

g is gravitational acceleration force (m s^{-2});

m_{sh} is mass of shaft (kg);

r_{sh} is reduce of shaft (m);

ω is angular velocity (rad s^{-1}).

For drum side torque calculations, the relation between speed and torque is used as Equation (26) (Khurmi and Gupta, 2005).

$$\frac{Tsr}{Tdr} = \frac{N2}{N1} \quad (26)$$

Where,

Tsr is torque on speed reducer pulley (Nm);

Tdr is torque on drum pulley (Nm);

N1 is motor speed (rpm);

N2 is speed at inlet of speed reducer (rpm).

$$Tdr = (T3\text{-}T4)\ r4 \quad (27)$$

Again, from Equations (22), (23), (26), and (27), the warp angle and lap angle for the drum side belt and pulley are determined as -2.063° and 3.214 rad, respectively. Then, from the belt tension Equation 24, *T3* was calculated as 126.3 N, and *T4* was 48.1 N.

Therefore, the load on the shaft due to the pulley

and belt was the sum of the tension on both sides and that of the pulley load. That is 1.5 kg pulley weight 1.5 x 9.81 = 14.71 N + 126.3 N + 48.1 N = 189.1 N was the weight exerted by the belt and pulley on the shaft. The other weight exerted on the shaft was the weight of the drum and the maximum weight of the cassava tuber loaded onto the machine. From section 2.6.1.2, the total mass of the drum was 26.8 kg, and the machine is designed to be loaded maximum of 15kg. Therefore, the weight due to the drum and cassava tubers was 41.8×9.81 = 410 N. In the shear force and bending moment diagram, the reaction force at points R1 and R2 corresponds to the bearing support and is determined as follows.

∑MR1=0 assume clockwise direction as positive.

$$R2 = 160.2N$$

$$\sum FY = 0$$

$$R1 = 438.9N$$

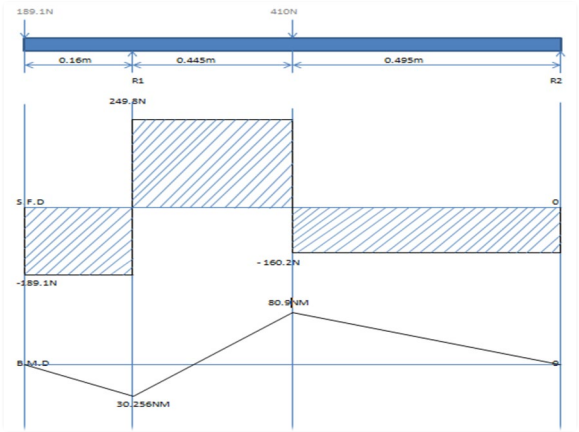

Figure 7 Shaft loading diagram for shear force and bending moment

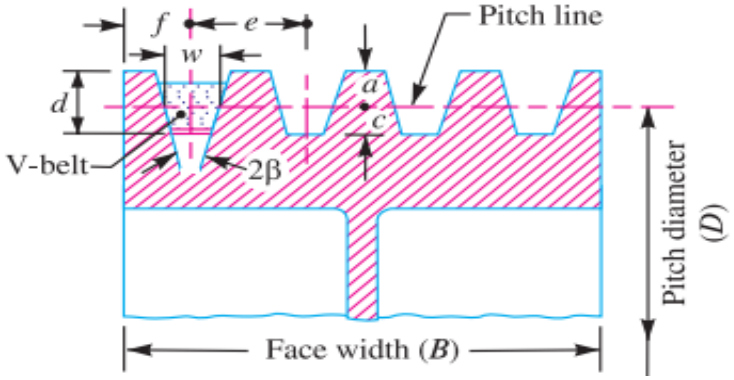

Figure 8 Cross-section of a v-groove pulley; the figure taken from (Khurmi and Gupta, 2005)

From the bending moment diagram, Mb = 80.9103 Nm, from the torque applied on the shaft, Mt = 3.910 Nm, and from equation 3.19, the diameter of the shaft can be calculated as.

$$d^3 = \frac{16}{\pi \tau all}\sqrt{(kb\ Mb)^2 + (kt\ Mt)^2}$$

d = 27.42mm ≈ 30mm

For the shaft with the keyway, the allowable stress τ should not exceed 40 MN m^{-2} (Khurmi and Gupta, 2005).

2.5.3 Design of pulley

Pulley was designed for a v-belt power transmission unit and so as to accommodate belt (see Figure 8) at any dynamic impulse of machine and speed variation according to classical v-belt was shown here. The maximum drum shaft pulley diameter is designed for 90 rpm speed of drum is 140mm while the intermediate pulley diameter is 100 mm for 60 rpm of drum shaft speed.

The drive pulley gives the horsepower rating at a maximum pitch diameter of pulleys and the corresponding speeds. The horsepower rating of the motor determines the diameter of the driver pulley. The shaft speed of the peeling drum and the speed of the prime mover-driven pulley were related by using Equation (28) (Khurmi and Gupta, 2005).

$$\frac{N1}{N2} = \frac{D2}{D1} \quad (28)$$

Where: *N1* is the angular speed of the motor (rpm), *N2* is the angular speed of the driven pulley (rpm), *D1* is the maximum pitch diameter of the driving or motor pulley (mm), and *D2* is the maximum pitch diameter of the driven or drum pulley (mm).

The width of the pulley (B) was usually considered to be 25% greater than the width of the belt (b), and Equation (29), as suggested by Richard and Nisbett (2011), was used to estimate the width of the pulley for the design of the intended cassava peeling

$$B = b + 0.25b = 1.25b \quad (29)$$

Where,

B is the Width of the pulley (mm) ;

b is the width of belt (mm) .

Table 1 Dimension of standard v-grooved pulley (all dimension in mm)

Types of belt	W	D	a	C	F	E	Groove angel (2β) degree
A	11	12	3.3	8.7	10	15	32, 34, 38

Source: Khurmi and Gupta (2005).

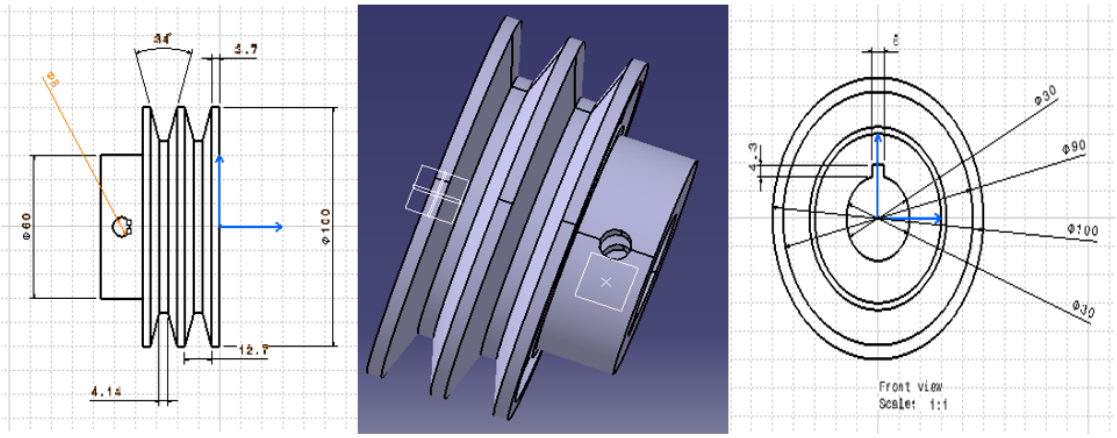

Figure 9 Pulley of the shaft

2.5.4 Design of Drum Cover

The drum cover was made from sheet metal of 1.5 mm thickness and 25 mm angle iron (90^0 shaped). It has the shape of a half cylinder and is used to protect the splash of peels from the operator and motor and to make the area clean from peels and debris.

2.5.5 Design of Protective Hood

The protective hood in Figure 11 was made from 1.5 mm sheet metal. It is used to protect splashing of dust and peels to the operator and motor. The angle of inclination was related to the repose angle of cassava peels.

2.5.6 Design of Frame

The frame supports the entire weight of the peeling machine. The total weights carried by the frame include the weight of the peeling drum, the weight of the cassava tuber, the weight of the drum cover, the weight of the shaft, the weight of the bearings, the weight of the pulleys and belt, and the weight of the protective hood. As shown below, the frame was rectangular in shape, 770 mm by 670 mm, and made from a hollow square section 40 x 40 x 4 mm, which can support the entire weight of the machine.

2.5.7 Belt selection

The belt used in transmitting power in the machine was selected considering type and dimension of standard V-belt according to ISO 4184. Based on Equation 30, a section belt having the belt code 50, an inner length of 1270mm, and an outer length of 1300mm for both the motor side and the drum side was chosen for the development of the machine. From section 2.6.2, the center distance between each pulley (see Figure 13) was calculated and the value obtained as presented in Table 2.

The nominal pitch length of the belt from an electric motor shaft to the speed reducer shaft and from the speed reducer shaft to the peeling drum shaft must be determined in order to know the actual belt size needed to transmit power from an electric motor

to the peeling drum. Therefore, according to Khurmi and Gupta (2005), the nominal pitch length "L" can be determined using Equation 30 for the motor side and Equation 31 for the drum side belt length, respectively.

$$L = 2X+\frac{\pi}{2}(D1+D2)+\frac{(D2-D1)^2}{4X} \quad (30)$$

$$L=2X+\frac{\pi}{2}(D3+D4)+\frac{(D4-D3)^2}{4X} \quad (31)$$

Where,

D1 is the diameter of the motor pulley (mm);

D2 is the diameter of the speed reducer pulley (mm);

D3 is the diameter of the speed reducer pulley (mm);

D4 is the diameter of the shaft pulley (mm);

X is the distance between the motor shaft pulley and the speed reducer shaft pulley for the motor side and the distance between the speed reducer shaft pulley and the drum shaft pulley (mm).

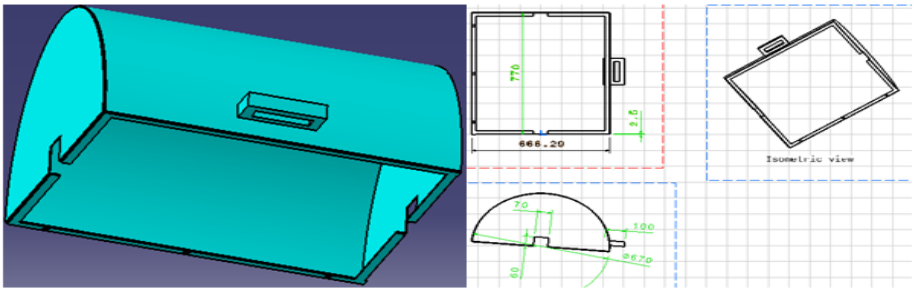

Figure 10 Drum cover

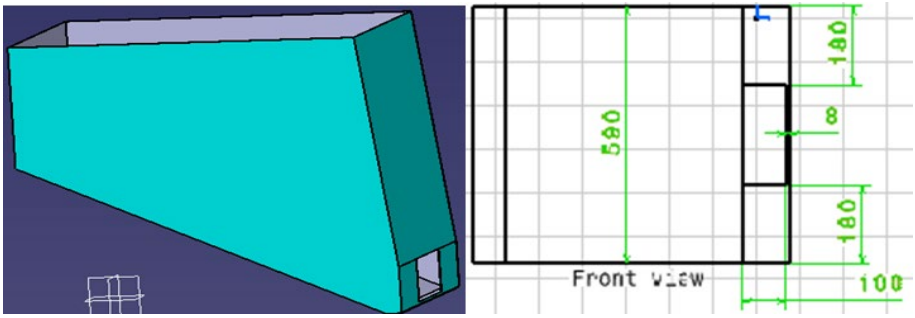

Figure 1 Protective hood

Power transmitted by V-belt and the velocity of the belt can be calculated using Equation (32) and (33) (Srivastava et al., 2006).

$$P = \frac{(T_1-T_2)V}{1000} \quad (32)$$

$$V = \frac{\pi \times d \times N}{60} \quad (33)$$

Where,

T1 and *T2* are tight-side and slack-side tension, respectively (N);

P is power transmitted (kW), *V* is belt speed (m s^{-1});

d is the diameter of the pulley at the motor (m);

N is the speed of the motor pulley (rpm).

But the power required to operate the peeling machine is the total sum of the power required to drive the peeling drum, the shaft, and the cassava tuber inside the drum, and the power required to overcome frictional force can be determined using Equation 34 (Nduka et al., 2012).

$$P_t=P+0.1P \quad (34)$$

Where: P_t is Total power (kW).

The number of belt required to transmit the power of motor to the drum can be determined using Equation (35) (Khurmi and Gupta, 2005).

$$\text{Number of belt required}=\frac{\text{total power transmitted}}{\text{power transmitted per belt}} \quad (35)$$

As a result of continuous runs of the belt over the pulleys there was a centrifugal force developed whose effect is to increase the tension of the belt on both the tight and slack side. However, according to Khurmi and Gupta (2005), if the speed of the belt is small (less than 10 m sec^{-1}), the effect of centrifugal tension is not considered. Equation (36) was used to determine centrifugal tension (Khurmi and Gupta, 2005).

$$T_c = mV^2 \quad (36)$$

Where,

Tc is centrifugal tension (N);

m is mass of belt (kg m^{-1});

V is velocity of belt (m sec^{-1}).

The tight side tension can be determined using Equation (37).

$$T_1 = T_{max} - T_c \quad (37)$$

Where,

T1 is the tight side belt tension (N);

Tmax is the maximum tension of the belt (N);

Tc is centrifugal tension (N).

The maximum tension of the belt, the mass of the belt, and the area of the belt are estimated using Equations 38-40, respectively, as suggested by Khurmi and Gupta (2005).

$$T_{max} = A\sigma \quad (38)$$

$$m = \rho A \quad (39)$$

$$A = \frac{(b-x)}{2}t + xt \quad (40)$$

A is the cross-sectional area of the belt (mm^2), σ is the maximum allowable stress of the belt (MPa), *b* is the top width of the belt (mm), *x* is the bottom width of the belt (mm), and *ρ* is the density of the belt (kg m^{-3}).

Power transmitted by V-belt (P= 0.38 KW) was determined using Equation 32 but the tension used to calculate the power was drum side tension that is *T3* and *T4*. The speed of the belt was given by Equation 33.

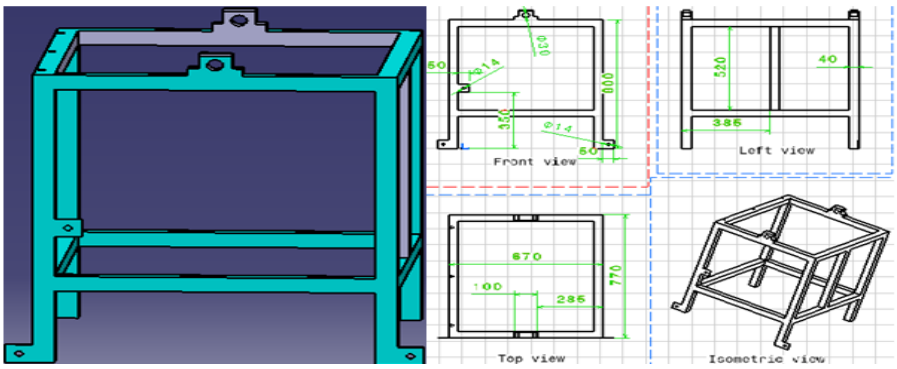

Figure 2 Frame

But, from Equation (34), it's known that total power was given by the relation

Pt = P + 0.1P→ Pt = 0.38 kw + 0.1x0.38 kw→Pt = 0.418

From Equation (35) the number of belts required to transmit the power of the motor was calculated as.

$$\text{Number of belt required} = \frac{\text{total power transmitted}}{\text{power transmitted per belt}} \quad (41)$$

$$\text{number of belt} = \frac{0.746}{0.418} \rightarrow \text{Number of belts} = 1.785 \approx 2$$

2.5.8 Bearing selection

A bearing was selected based on its load-carrying capacity, life expectancy, and reliability. The size and type of bearing were determined after the determination of required radial load, thrust load, diameter of shaft and desired life. While selecting bearings, we have to be familiar with bearing codes as shown in Table 3.

2.5.9 Selection of electric motor

An electric motor for Casava peeler machine operation was selected by considering its reliability, endurance, working environment, speed, and power. Since the operation of the machine is for a small scale and the inherent motor speed range for such operation is 1450-1500 rpm, 1450 rpm speed motor was selected. The motor power required for small and medium operation ranges is 1 to 2 hp, and 5 to 10 hp for industrial purposes. 1hp motor was selected which required 220 volts with rated frequency of 50Hz and 1.5-465A current. The selected electrical motor has a model number YL-802, which is locally available and reliable in operation.

2.6 Experimental procedure

The cassava was sorted out based on length and cut to an average length of 30 cm; six pulley sizes (two 86 mm, two 100 mm, and two 140 mm) were used for speed variation of 30 rpm, 60 rpm, and 90 rpm. The machine was run using 90 rpm arrangement of the pulleys' size and it was observed that the speed was high and no peeling was performed at different feed rate for predetermine retention time. Then the drums were rotated by a pulley arrangement of 30 rpm and 60 rpm at different feed rates and specified retention times, and the cassava tubers started to be peeled. Hence, slow speed was decided to be better for the machine operation, achievable by using a speed reduction gear.

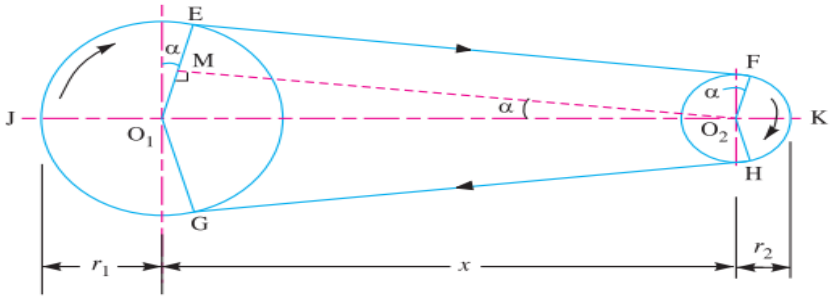

Figure 3 Belt expiration

Table 2 Dimension of standard v-belt according to IS: 2494-1974

Types of belt	Power ranges KW	Minimum pitch diameter of pulley (D) mm	Top width (b) mm	Thickness (t) mm	Weight per meter length in newton
A	0.7-3.5	75	13	8	1.06

Source: Khurmi and Gupta (2005).

Table 3 Radial bearing numbers and their implication

Bearing code No.	Bore (mm)	Outside diameter	Width (mm)
206	30	62	16
306		72	19
406		90	23

Source: Khurmi and Gupta, 2005.

2.7 Performance evaluation of cassava peeler machine

The experiment was conducted using a split-plot design, with drum speed as the main plot and the percentage of drum fill as sub-plots. The experiment was repeated three times, resulting in a total of 18 experimental units (2x3x3=18). The independent variables were drum speed (30 rpm and 60 rpm) and percentage drum fill (10%, 15%, and 20%), while the dependent variables included peeling efficiency (%), throughput capacity (kg h^{-1}), percentage mass of flesh loss, percentage mass of peeled cassava, percentage mass of cassava peels, and percentage mass of unpeeled cassava.

A total of 195 kg of fresh cassava tubers of the Hinda variety were used for the entire test run. A predetermined mass of cassava tubers was loaded into the peeling drum and rotated at a specified drum speed for 7 minutes. The machine's performance was then evaluated based on peeling efficiency, throughput capacity, and flesh loss as shown in Figure 14.

Peeling efficiency was measured by comparing the mass of cassava peels collected at the machine's outlet and the mass of peels removed by hand after machine peeling, determined using Equation (42). Throughput capacity was calculated based on the mass of cassava peeled within a specific time using Equation 43. The percentage mass of flesh loss was estimated using Equation 44, based on the proportion of flesh lost with peels relative to the total peeled mass minus the peels removed by hand. The percentage mass of peeled cassava was determined

using Equation (45), considering the proportion of cassava tubers peeled by the machine relative to the total cassava fed. The percentage mass of cassava peels, removed by both machine and hand, was calculated using Equation (46). The percentage of unpeeled cassava was estimated by comparing the mass of unpeeled cassava to the total cassava mass using Equation (47). Finally, an economic analysis of the developed cassava tuber peeler machine was performed, considering the machine's cost and the benefit-cost ratio.

Figure 14 Performance testing of peeling machine

$$\text{Peeling efficiency(n)} = \frac{M_{pls}}{M_{prh}+M_{pls}} \times 100 \text{ (Fadeyibi and Ajao, 2020)} \quad (42)$$

$$\text{Throughput(Tc)} = \frac{M_t}{T} \quad (43)$$

$$\%\text{mass of flesh loss} = \frac{M_f}{M_{tf}} \times 100 \text{ (Fadeyibi and Ajao, 2020)} \quad (44)$$

$$\%\text{mass of peeled cassava} = \frac{M_p}{M_t} \times 100 \text{ (Ebomwomyi et al., 2017)} \quad (41)$$

$$\%\text{mass of peels of cassava} = \frac{M_{pls}+M_{prh}}{M_t} x100 \text{ (Ebomwomyi et al., 2017)} \quad (46)$$

$$\%\text{mass of unpeeled cassava} = \frac{M_u}{M_t} \times 100 \text{ (Ebomwomyi et al., 2017)} \quad (47)$$

Where,

M_t is the mass of cassava fed to the machine in (kg);

T is the time taken for cassava and its peels to completely leave the machine in hours;

M_{pls} is the mass of cassava peels collected at the outlet of the machine in (kg);

M_{prh} is the mass of cassava peels removed by hand after machine peeling in (kg);

M_f is mass of cassava flesh lost removed along with the peels by the machine in (kg);

M_{tf} is total mass of flesh tubers in kg;

M_p is Mass of completely peeled cassava (kg);

M_u is mass of unpeeled cassava in (kg).

3 Result and discussion

3.1 Performance of cassava peeler machine

The cassava tuber peeler machine was tested under varying conditions of drum speed and percentage drum fill to determine its performance in terms of peeling efficiency, throughput capacity, and percentage mass of flesh loss.

3.1.1 Peeling efficiency analysis

The results of the regression analysis showed that 65.3% of peeling efficiency was accounted by two factors collectively, F (2, 15) = 17.025, p = 0.00, confirming that these factors influence peeling efficiency.

Looking at individual contribution of the predictors, the result showed that peeling drum speed (β = 0.747, t = 5.228, p = 0.00) positively affect the peeling efficiency while the percentage of drum fill (β = -0.37, t = -2.591, p = 0.02) negatively affect the peeling efficiency of the developed cassava peeler machine, meaning that increasing the drum fill reduces efficiency (see Table 5).

The predicted model for peeling efficiency is:

$$n = 75.484 + 8.772\ (PDS) - 2.633\ (DF)$$

The coefficient 8.772 associated with *PDS* indicates that for every one-unit increase in peeling drum speed (rpm), the peeling efficiency increases by 8.772%, assuming the percentage drum fill remains unchanged. This positive effect suggests that a higher drum speed improves the machine's efficiency. Conversely, the coefficient -2.633 for DF signifies that for every 1% increase in drum fill, the peeling efficiency decreases by 2.633%, assuming PDS remains constant. This negative impact suggests that increasing the drum fill reduces efficiency, possibly due to overcrowding in the drum, which limits effective contact between the peeling surface and cassava. Overall, the model suggests that peeling efficiency improves with higher drum speed but declines with increased drum fill, providing insights for optimizing machine performance.

From Table 8**,** throughput capacity increased from 60 kg h^{-1} (10% fill) to 120 kg h^{-1} (20% fill) at both 30 rpm and 60 rpm, showing that throughput is highly dependent on drum fill rather than speed**.**

In conclusion, as the higher peeling drum speed improves peeling efficiency due to increased friction and abrasion on cassava tubers, while increasing the percentage of drum fill reduces peeling efficiency because excessive tubers restrict movement and reduce effective contact with the peeling surface. Therefore, the optimal condition for maximum peeling efficiency is 60 rpm with 10% drum fill (94.87% efficiency).

Table 4 Regression analysis for peeling efficiency

Hypothesis	Regression	weight	Beta	Coefficient	t-value	p-value	Hypothesis supported
H_1	PDS →	n		0.747	5.228	0.00	YES
H_2	DF →	n		-0.37	-2.591	0.02	NO

Table 5 Effect of peeling drum speed and drum fill on peeling efficiency

Hypothesis	Predictor (IV)	Dependent Variable (DV)	Regression Coefficient	Beta	t-value	p-value	Supported
H1: (PDS) → (n)	(PDS)	(n)	8.772	0.747	5.228	0.00	Yes
H2:(DF)→ (n)	(DF)	(n)	-2.633	-0.37	-2.591	0.02	No

Where: H_1 and H_2 are hypotheses 1 and 2, respectively, PDS is peeling drum speed, n is peeling efficiency, and DF is percentage drum fill.

3.1.2 Throughput capacity analysis

The regression analysis showed that 96% of the variation in throughput capacity was explained by the two independent variables **(**F (2,15) = 26.667, p = 0.00**).** The regression analysis showed that 96% of the throughput capacity was varied by two independent factors collectively, F (2, 15) = 26.667, p = 0.00.

Looking at individual contribution of the predictors, the result showed that peeling drum speed (β = 0.00, t = 0.00, p = 1.00) has no effect on throughput capacity while the percentage of drum fill (β = 0.982, t = 20.125, p = 0.00) which indicates a strong positive impact of drum fill on throughput capacity as shown in Table 6.

The predicted model for throughput capacity is:

$$TC = 26.667 + 0.00\ (PDS) + 30.00\ (DF)$$

Meaning that the peeling drum speed (PDS) does not affect throughput capacity because the coefficient is 0.00. No matter how much PDS changes, the throughput capacity remains unaffected but for every 1% increase in the Percentage Drum Fill (DF), the throughput capacity increases by 30 units.

Table 6 Effect of peeling drum speed and drum fill on throughput capacity

Hypothesis	Predictor (IV)	Dependent Variable (DV)	Regression Coefficient	Beta	t-value	p-value	Supported
H1: (PDS) → (TC)	(PDS)	(TC)	0.00	0.00	0.00	1.00	No
H2: (DF) → (TC)	(DF)	(TC)	30.00	0.982	20.125	0.00	Yes

Where: H1 and H2 are hypotheses 1 and 2, respectively.

PDS is peeling drum speed, TC is throughput capacity, and DF is percentage drum fill.

Table 7 Effect of peeling drum speed and drum fill on percentage mass of flesh loss

Hypothesis	Predictor (IV)	Dependent Variable (DV)	Regression Coefficient	Beta	t-value	p-value	Supported?
H1: (PDS) → (MF)	(PDS)	(MF)	3.367	0.799	6.165	0.00	Yes
H2: (DF) → (MF)	(DF)	(MF)	-0.85	-0.33	-2.542	0.023	No

Where: H1 and H2 refer to hypothesis 1 and hypothesis 2**,** respectively. PDS is peeling drum speed**,** MF is percentage mass of flesh loss**,** and DF is percentage drum fill**.**

Table 8 The effect of independent variables over dependent variables

Descriptive Statistics					
	Drum speed	drum fill	Mean	Std. Deviation	N
peeling efficiency (n) in %	30rpm	10%	77.9667%	3.36204%	3
		15%	79.4667%	0.64291%	3
		20%	79.3500%	0.31225%	3
	60rpm	10%	94.8667%	0.90738%	3
		15%	85.4000%	0.98489%	3
		20%	82.8333%	1.15902%	3
% mass of flesh loss	30rpm	10%	2.200	0.3606	3
		15%	3.433	0.3786	3
		20%	2.567	0.3215	3
	60rpm	10%	7.800	1.0440	3
		15%	6.467	0.4726	3
		20%	4.033	0.7506	3
Throughput capacity (Tc) in kg h^{-1}	30rpm	10%	60.00	0.000	3
		15%	80.00	0.000	3
		20%	120.00	0.000	3
	60rpm	10%	60.00	0.000	3
		15%	80.00	0.000	3
		20%	120.00	0.000	3

From Table 8, throughput capacity increased from 60 kg h^{-1} (10% fill) to 120 kg h^{-1} (20% fill) at both 30 rpm and 60 rpm, showing that throughput is highly dependent on drum fill rather than speed**.**

The point could be taken here is, the throughput capacity of the cassava peeling machine is primarily influenced by the percentage of drum fill rather than the peeling drum speed. Therefore, to balance throughput and efficiency, an optimal setting is 60 rpm with 15% drum fill, where throughput reaches 80 kg h^{-1} while maintaining a relatively high peeling efficiency of 85.4%.

3.1.3 Percentage Mass of Flesh Loss Analysis

The regression results showed that 71.4% of the percentage flesh loss was caused due to the two independent variables collectively, $F(2, 15) = 22.234$, $p = 0.00$.Looking at individual contribution of the predictors, the result showed that peeling drum speed ($\beta = 0.799$, $t = 6.165$, $p = 0.00$) positively affect the percentage flesh loss indicates that higher drum speeds significantly increase flesh loss while the percentage of drum fill ($\beta = -0.33$, $t = -2.542$, $p = 0.023$) negatively affect the percentage mass of flesh loss of cassava peeler machine suggests that higher drum fill reduces flesh loss as shown in Table 7.

The predicted model for the percentage mass of flesh loss is:

$$MF = 1.067 + 3.367\,(PDS) - 0.85\,(DF)$$

This indicates that for every unit increase in peeling drum speed (PDS), the mass of flesh loss increases by 3.367%, assuming DF remains constant, while for every unit increase in percentage drum fill (DF), the mass of flesh loss decreases by 0.85%, assuming PDS remains constant. From Table 7, flesh loss was highest **(**7.8%**)** at 60 rpm and 10% drum fill**,** while it decreased to 2.2% at 30 rpm and 10% drum fill**.**

Therefore, since the flesh loss increases with drum speed due to excessive friction, leading to over-peeling and the reduction in flesh loss with increasing drum fill may be due to reduced direct contact between tubers and the peeling surface, to minimize flesh loss while maintaining good peeling efficiency, 60 rpm with 15% fill is recommended.

3.1.4 Summary of the effects of independent variables

Based on the above analysis and the data in Table

8, a trade-off between efficiency, throughput, and flesh loss indicates that an optimal combination of drum speed and drum fill is necessary to maximize peeling performance while minimizing flesh loss. So, a peeling drum speed of 60 rpm and a 15% drum fill is suggested because this will allow for high peeling efficiency (85.4%) while still maintaining a good throughput and at an acceptable level of flesh loss. This setting provides a peeling efficiency of 85.4%, a throughput of 80 kg/h, and a flesh loss of 6.467%. The flesh loss at 15% drum fill is lower than the 7.8% observed at 10% drum fill, making it an acceptable level while maintaining a reasonable throughput. Although further reducing flesh loss is possible at 20% drum fill, it comes at the expense of peeling efficiency, making the 15% drum fill setting the most balanced choice.

4 Conclusion

This study focused on the design, development, and performance evaluation of an electrically operated cassava peeling machine to solve the problems encountered in cassava peeling processes. An electrically operated cassava peeling machine was designed, developed, tested and evaluated. The cassava peeling machine has a rotating drum with an opening inlet and outlet door, a protective hood (drum cover and means to guide peels out) and motor setup and supporting frame.

The performance of the developed cassava peeling machine was evaluated in terms of peeling efficiency (%), mass of flesh loss (%) and throughput capacity (kg hr^{-1}). The test was carried out at 30 and 60 rpm peeling drum speed and 10%, 15% and 20% percentage drum fill by holding the operation at 7 minutes.

The maximum peeling efficiency of 94.8667% of the developed cassava peeling machine was recorded when the machine was operated at 60rpm drum speed, 10% drum fill and 7-minute retention time. At this operating condition percentage mass of flesh loss and throughput capacity were found to as 7.8% and 60 kg h^{-1} respectively. The maximum throughput capacity of 120 kg hr^{-1} was recorded at 20% drum fill, independent of drum speed. The maximum tuber flesh loss of 7.8% on the other hand, was recorded when drum speed was 60rpm and the drum is filled 10%. Table 11 shows the summary of the findings.

There was a direct relationship between percentage drum fill and throughput capacity, however, the relationship between peeling drum speed and peeling efficiency, percentage drum fill and peeling efficiency, peeling drum speed and percentage mass of flesh loss and percentage drum fill and percentage mass of flesh loss was not directly interrelated. Testing and performance evaluation of developed cassava peeler machine were conducted to determine the effect of peeling drum speed and percentage drum fill on peeling efficiency, percentage mass of flesh loss and throughput capacity of the machine by keeping retention time constant. The optimum operating conditions were determined at 60 rpm of peeling drum speed and 10% of drum fill based on the goal of maximize peeling performance while minimizing flesh loss.

Acknowledgments

The authors gratefully acknowledge the financial support from Adama Science and Technology University and Malkasa Agricultural Research Center for technical support.

Conflict of interest

The authors declare that they have no known competing financial interests or personal relationships that could have appeared to influence the work reported in this paper.

References

Alhassan, E. A., O. J. Ijabo, and E. O. Afolabi. 2018. Development of cassava peeling machine using an abrasive mechanism. *Journal of Production Engineering*, 21(1): 61-66.

Amsalu. A. 2006. Phenotypic Diversity of Cassava (Manihot esculenta Cranz.) in Ethiopia. In *Proceedings of the*

12th Annual Conference of the Crop Science Society of Ethiopia, 23-29. Addis Ababa, May 22-24.

Aniedi, O. E., O. A. Linus, A. E. Ime, and E. Benjamin. 2012. Mechanization of cassava peeling. *Journal of Research in Engineering and Applied Sciences*, 1(5): 334-337.

Davies, R. M., M. O. Olatunji, and W. Burubai. 2008. Mechanization of cassava processing in Iwo Local Government Area of Osun State, Nigeria. *World Journal of Agricultural Sciences*, 4(3): 341-345.

Ebomwomyi, P., E. M. Oroh, E. G. Sadjere, and G. O. Ariavie. 2017. Design of an improve cassava peeling machine. *International Journal for Research in Applied Science & Engineering Technology* (IJRASET), 5(6): 1718-1723.

Ehiem, J. C., and K. J. Simonyan. 2012. Physical properties of willed mango fruits and nuts. *International Agrophysics*, 26(1): 95-98.

Ertebo, A. E., and A. W. Koroso. 2024. Design and manufacturing of cassava grater machine. *CIGR Journal*, 26(4): 73-90.

Fadeyibi. A., and O. F. Ajao. 2020. Design and performance evaluation of a multi-tuber peeling machine. *AgriEngineering*, 2(1): 55-71.

Gezahegn, A., and M. Bazie. 2021. Cassava production, processing and utilization in South Western part of Ethiopia. *Asian Research Journal of Agriculture*, 14(1): 57–63.

Hughes, S. W. 2005. Archimedes revisited: a faster, better, cheaper method of accurately measuring the volume of small objects. *Physics Educatio*n, 40(5): 468-474.

Immanuel, S., D. Jaganathan, P. Prakash, and S. Sivakumar. 2024. Cassava for Food Security, Poverty Reduction and Climate Resilience: A Review. *Indian Journal of Ecology*, 51(1): 21-31.

Kanaabi, M., M. B. Settumba, E. Nuwamanya, N. Muhumuza, P. Iragaba, A. Ozimati, F. B. Namakula, I. S. Kayondo, J. K. Baguma, A. R. Nanyonjo, W. Esuma, and R. S. Kawuki. 2024. Genetic Variation and Heritability for Hydrogen Cyanide in Fresh Cassava Roots: Implications for Low-Cyanide Cassava Breeding. *Plant*s, 13(9): 1186.

Khurmi, R. S., and J. K. Gupta. 2005. *A Textbook of Machine Design*. New Delhi, India: Eurasia Publishing House.

Koocheki, A., S. M. A Razari, E. Milani, T. M. Abedin. M. Abedini, S. Alamatiyan, and S. Izadikhah. 2007. Physical properties of watermelon seed as a function of moisture content and variety. *International Agro Physics*, 21(4): 349-359.

Markos, D., L. Hidoto, and F. Negash. 2016. Achievements of Cassava Agronomy Research in Southern Ethiopia in the Last two Decades. *Agriculture and Food Sciences Researc*h, 3(1): 12-18.

Ndirika, V. I .O., and O. O. Oyeleke. 2006. Determination of selected physical properties and their relationships with moisture content for millet (Pennisetum Glaucum L). *Applied Engineering in Agricultur*e, 22(2): 291-297.

Nduka, N. B., O. A. Okay, and A. C. Jonah. 2012. Design, fabrication and evaluation of palm nut-pulp separator. *Journal of Emerging Trends in Engineering and Applied Sciences*, 3(1): 144-151.

Rao, M. A., S. S. H. Rizvi, A. K. Datta, and J. Ahmed. 2014. *Engineering Properties of Foods*. 4th ed. Boca Raton, FL, USA: CRC Press.

Sakadzo, N., A. T. Kugedera, N. Ranganai, and L. K. Kokerai. 2025. Cassava: practices and technologies to improve food security in sub-Saharan Africa. *Cogent Food and Agriculture*, 11(1): 2518758.

Sarka, S., D. Woldeyohannes, and A. Woldesilasie. 2017. Value chain analysis of cassava in Wolaita Zone, SNNPR, Ethiopia. *Journal of Economics and Sustainable Development*, 8(5): 11-17.

Scaria, S. S., B. Balasubramanian, A. Meyyazhagan, J. Gangwar, J. P. Jaison, J. T. Kurian, K. Pushparaj, M. Pappuswamy, S. Park, and K. S. Joseph. 2023. Cassava (*Manihot esculenta* Crantz)- A potential source of phytochemicals, food, and nutrition: An updated review. *E-Food*, 5(1): e127.

Srivastava, A. K., C. E. Goering, R. P. Rohrbach, and D. R. Buckmaster. 2006. Mechanical Power Transmission. In ,*Engineering Principles of Agricultural Machine*, 2nd ed, eds. A. K, Srivastava, C. E. Goering, R. P. Rohrbach, and D. R. Buckmaster, ch. 4. 65-90. St. Joseph, Michigan: ASABE.

Tobiloba, O., K. Oluwaseun, and R. O. Leram. 2019. Performance of cassava peeling machines in Nigeria: A review of literature. *Journal of Physics: Conference Series*, 1378(2): 022084.

Ukonu, C. U., H. O. Lasisi, E. A. Adewole, and J. H. Olunaike. 2022. Empirical Analysis of Hydrogen Cyanide in Streams used for Commercial Fermentation of Cassava. *American Journal of IT and Applied Sciences Research*, 1(3): 1-9.

Wilson, W. M., and D. L. Dufour. 2002. Why “bitter” cassava? The productivity of “bitter” and “sweet” cassava in a Tukanoan Indian settlement in the Northwest Amazon. *Economic Botan*y, 56(1): 49-57.